The EMBO Journal vol.8 no.11 pp.3523 - 3533, 1989

Heteroduplex substrates for bacteriophage lambda site-specific recombination: cleavage and strand transfer products

Howard A.Nash and Carol A.Robertson

Laboratory of Molecular Biology, National Institute of Mental Health, 9000 Rockville Pike, Building 36, Room 1B-08, Bethesda, MD 20892, USA

Communicated by D.Sherratt

Lambda's Int protein acts as a specific topoisomerase at attachment sites, the DNA segments that are required for site-specific recombination. Int cleaves each strand of an attachment site at a unique place and creates strand exchanges by joining broken ends from two different parents. To study the action of Int topoisomerase in more detail, heteroduplex attachment sites were made by annealing strands that are complementary except for a few base pairs that lie in the region between the points of top and bottom strand exchange in the attachment site core. These heteroduplexes appear to interact normally with Int and its accessory proteins IHF and Xis. Although the heteroduplex sites are specifically cleaved by Int topoisomerase, rejoining of the broken DNA is hindered by the lack of Watson–Crick complementarity adjacent to the break. Because of this, heteroduplexes accumulate broken intermediates which are then processed in novel ways. We have used this feature to provide new information about functional differences between attachment sites, to investigate the way Xis protein controls directionality of site-specific recombination, and to demonstrate that Int protein can join strands indiscriminately and can therefore generate recombinants with either of two genetic polarities.

Key words: bacteriophage lambda/recombination/topoisomerase

Introduction

The hallmark of the reaction that joins the chromosomes of bacteriophage lambda and *Escherichia coli* is site-specificity, i.e. integration takes place by recombination between a unique locus on the phage DNA and a unique locus on the bacterial DNA (Campbell, 1962). These loci are called attachment sites and are now understood to have the following structure (reviewed in Weisberg and Landy, 1983). The segment at which the joining takes place, called the overlap region and designated by the symbol O, has the same sequence in the phage attachment site, *att*P, and the bacterial attachment site, *att*B. Flanking this crossover region are elements that are essential for attachment site function; these differ from each other between phage and bacterial sites and between the left and right sides of O. Thus, the equation for lambda integration can be written: POP′ + BOB′ → BOP′ + POB′. The recombinant sites BOP′ and POB′ are named *att*L and *att*R because they form, respectively, the left and right boundaries of the integrated viral DNA or prophage. The equation emphasizes the fact that lambda integration involves a reciprocal genetic exchange in the overlap region that rearranges the flanking elements. In the lambda system genetic exchange is known to be conservative in that no external energy source is needed. As implied by this conservation of energy, breakage and reunion proceed by a topoisomerase mechanism. Specifically, lambda's Int protein cleaves one strand within each attachment site and covalently joins to the broken end. A Holliday junction is formed when Int releases its hold on the broken DNA and simultaneously rejoins cleaved strands from two attachment sites; resoluton of the Holliday junction to a completed recombinant occurs when the remaining pair of strands are broken and rejoined by Int topoisomerase. In between formation and resolution, the Holliday junction is thought to migrate across the overlap region, a process which would explain the requirement that two attachment sites must have perfect homology throughout this short region in order to recombine efficiently. Thus, in its elemental form, lambda integration is merely a multi-step topoisomerase transaction. However, the strucure of the attachment sites implies further complexity.

Each attachment site contains an array of binding sites for recombination proteins (reviewed in Craig, 1988). Common to all attachment sites is a pair of inversely repeated binding sites for Int protein. Binding to these sites positions the topoisomerase function of Int protein so that it can initiate strand exchange by cleavage at the edge of the overlap region. (In this work we use the term core to signify the ~30 bp segment of DNA that contains the primary elements of strand exchange, i.e., a pair of inversely repeated Int binding sites and the DNA between them. The term overlap signifies the 7 bp segment of the core that separates the points of top and bottom strand exchange.) The four so called core or junction binding sites for Int have subtly different sequences from one another. However, Nunes-Düby *et al.* (1987) have shown that artificial attachment sites in which all core binding sites are identical can recombine efficiently with each other; the natural differences thus appear to be incidental. Beyond the core region, in the so called arms of the attachment site, differences between sites are highly significant. *att*B contains no important binding sites in its arms; the bacterial DNA appears to consist simply of an overlap region flanked by an inverted pair of core sites. In contrast, the P and P′ elements of *att*P contain many binding sites that are critical for function. Both P and P′ contain additional binding sites for Int protein [recognized by a domain of Int that is different from the one which recognizes the core sites (Moitoso de Vargas *et al.*, 1988)] and binding sites for IHF, an *E.coli* protein that assists in the proper folding of *att*P by bending DNA (Robertson and Nash, 1988; Thompson and Landy, 1988). The P arm also contains binding sites for Xis, a viral protein that controls the directionality of the recombination and binding sites for Fis, an *E.coli* protein that assists the binding of Xis. Xis controls

directionality of recombination both by inhibiting integration and by activating excision of the prophage, i.e. recombination between *att*L and *att*R. The mechanism by which Xis alters the efficiency of these reactions remains to be determined.

Since arm sites control the efficiency and directionality of recombination, we would like to know about functional interactions between proteins bound to the arms and cores of attachment sites. One way in which this can be done is to examine the topoisomerase action of Int when bound to the core and ask how it is affected by the presence of binding sites in the arms. Such an assay complements footprinting assays not only because it can be more sensitive but because it can provide information on the functional state of a bound protein. Our assay utilizes the finding that Int topoisomerase can be detected uncoupled from recombination (Craig and Nash, 1983) and the observation that detection of this activity can be greatly enhanced with attachment site substrates containing mismatches in the overlap region (Nash *et al.*, 1987a; see below for details). In the past we have used these assays to provide critical information about the behavior of *att*B during integrative recombination (Nash *et al.*, 1987a; Richet *et al.*, 1988). We have now extended our studies with heteroduplex attachment sites. We have analyzed the effect of the P arm on the interaction of Int with the cores of *att*P (POP′) and *att*R (POB′), have studied the capacity of Xis protein to alter attachment site function and have determined the structure of cleaved and rejoined products. In the course of these studies, we have uncovered a surprising strand exchange product, one which is not predicted by classical genetic schemes and is indicative of a previously unsuspected flexibility in lambda strand exchange function. Using a radically different approach, the replacement of a normal attachment site by one that is pre-cleaved in the overlap region, Nunes-Düby *et al.* (1989) have come to conclusions similar to ours about the participation of Xis protein in site-specific recombination and the capacity of Int topoisomerase to rejoin unrelated strands.

Results

Experimental strategy

The fundamental advantage of using heteroduplex attachment sites as substrates for Int topoisomerase assays is diagrammed in Figure 1. With a homoduplex substrate (Figure 1A), a small amount of cleavage can be detected upon incubation with Int (Craig and Nash, 1983). The low yield of this reaction reflects not only the lack of coupling to a recombination partner but also the tendency of topoisomerases to reseal cleaved DNA as part of the cycle of breakage and reunion. This tendency is inhibited when the substrate of Figure 1B is used. Here, a heteroduplex attachment site has been assembled by annealing strands that contain different DNA sequences in the overlap region. Attachment sites with differing overlap sequences were first isolated by Weisberg *et al.* (1983). These variants are called *saf* mutants; the one we employ, *saf*G, has three changes from the 7 bp wild-type overlap sequence. Thus, the heteroduplexes in this work have three mismatched pairs between the points where Int cleaves the top and bottom strands. When Int cleaves such a heteroduplex attachment site rejoining should be diminished because, in the absence of Watson–Crick pairing, the strand ends are not held in close proximity (Figure 1B). If both strands suffer topoisomerase cleavage, the attachment site falls apart. In earlier work, we were surprised that the mobility of such half-attachment sites showed no indication of the covalently

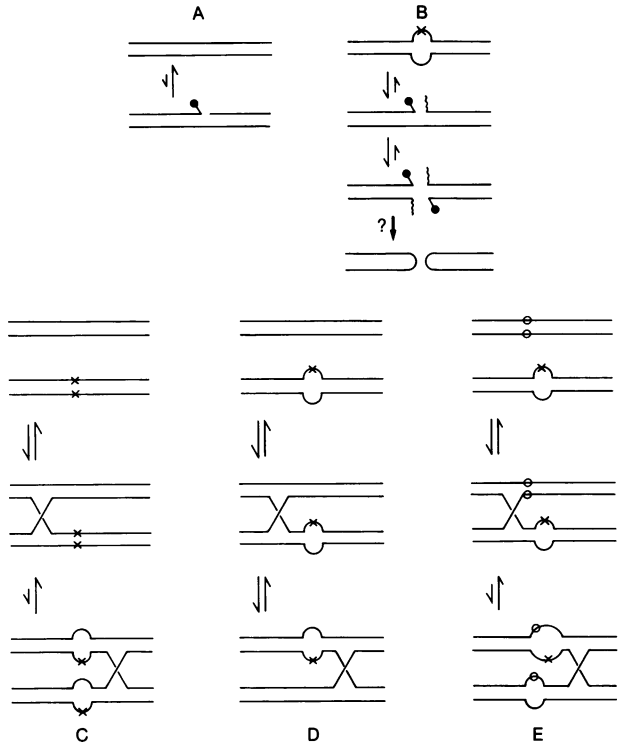

Fig. 1. Cleavage and strand transfer with homoduplex and heteroduplex attachment sites. (**A**) A simple homoduplex attachment site (**top**) undergoes limited cleavage upon incubation with Int. Either strand is cleaved inefficiently; double-strand breaks are even rarer but do occur. Each cleavage leaves a free 5′ hydroxyl end but the 3′ phosphate end has a covalently attached Int protein (solid circle). (**B**) A heteroduplex site (**top**) has been constructed by annealing a wild-type attachment site and a *saf* variant (base changes in the variant indicated by an x). Cleavage by Int can be more pronounced than in **panel A** because resealing is inefficient. Double-strand breakage is postulated to form hairpins (**bottom**) as a result of a misguided attempt by Int topoisomerase to complete strand transfer. (**C**) The top panel pictures homoduplex attachment sites that have been juxtaposed during synapsis; one of the sites is a *saf* variant (position of the non-homology marked with x's). Strand exchange to form a Holliday junction and branch migration are as described in the text. Because of the unfavorable energy cost associated with formation of mismatched base pairs, branch migration is strongly disfavored and few joints reach the end of the overlap region (**bottom**). Consequently, little or no completed recombinant is generated. (**D**) Synapsis (**top**), Holliday junction formation (**middle**) and branch migration (**bottom**) are all efficient when a heteroduplex substrate is used, provided one strand of the heteroduplex (the one not marked with an x) is identical to one of the strands of the recombination partner. As a result, completed recombinants accumulate in this assay. These recombinant products may be subject to subsequent double-strand cleavage if recombination converts a site that binds Int poorly into one that binds Int well (Nash *et al.*, 1987a). (**E**) The homoduplex attachment site carries a different *saf* mutation (marked by circles) than that used to generate the heteroduplex (marked by an x). Synapsis (**top**) and formation of Holliday joints (**middle**) may proceed normally, but branch migration (**bottom**) should again be disfavored by creation of additional mismatched pairs. Because two closely spaced mismatches are not expected to require twice as much energy as either single mismatch, the blockage to branch migration may not be as severe as that shown in **panel C**. Thus, although recombinant products have been reported to be depressed in several cases (Bauer *et al.*, 1985; Nash *et al.*, 1987a) the degree of depression should vary with the particular *saf* combination tested. Even if strand transfer is very inefficient, synapsis may be detected by the stimulation of double-strand cleavage of the heteroduplex substrate (Richet *et al.*, 1988).

bound Int protein (Nash *et al.*, 1987a). As diagrammed in the bottom panel of Figure 1B, this could be explained by the rejoining of complementary strands into hairpins.

Although some heteroduplex sites are very efficiently cleaved upon incubation with Int, others are not, presumably because of a weak interaction of Int with the core. In these cases, it is useful to assess the performance of the heteroduplex as a substrate for a recombination reaction. To understand the behavior of heteroduplex sites in such assays, consider first recombination with homoduplex attachment sites (Figure 1C). The sites come together during synapsis (top), exchange one pair of strands to form a Holliday junction (middle), and branch migrate across the overlap region (bottom) prior to resolution of the Holliday junction (not shown). In the example of Figure 1C the sequence of the overlap region of one attachment site differs from that of the other, i.e. one site is a *saf* mutant. Branch migration would therefore generate two non-Watson–Crick pairs. Although crosses between two attachment sites with the identical *saf* mutation are perfectly efficient, crosses between wild-type and *saf* attachment sites yield little or no completed recombinants. As first suggested by Weisberg *et al.* (1983), we believe that the cost of forming two non-Watson–Crick pairs upon branch migration explains this outcome. The amount of Holliday structure seen in such crosses is low, suggesting that such junctions are unstable intermediates and readily undergo strand exchange back to the parental configuration (Kitts and Nash, 1987). Indeed, efficient processing of artificial Holliday junctions by Int protein has been observed (Hsu and Landy, 1984; de Massy *et al.*, 1989). When heteroduplex substrates undergo strand exchange, a different balance of forces applies during branch migration. If, as shown in Figure 1D, one strand of the heteroduplex is identical to one strand of the recombination partner (e.g. both come from *saf*$^+$), branch migration generates no additional non-Watson–Crick pairs. This scheme explains the observation that heteroduplex attachment sites yield completed recombinants with the same speed and efficiency as fully homologous homoduplex substrates (Bauer *et al.*, 1984; Nash *et al.*, 1987a). The substrates diagrammed in Figure 1E represent another interesting case. Here, there is both a non-homology in the homoduplex portion of the overlap region as well as a heteroduplex in an adjacent portion of the overlap region. As diagrammed, branch migration should again increase the total number of mismatched base pairs and should therefore be inefficient. However, in this case, even if Holliday junctions are resolved back to original substrates as described in Figure 1C, there is an improved opportunity to discover that some attempt at recombination has taken place. This is because the heteroduplex can show enhanced cleavage in the presence of a recombination partner (Richet *et al.*, 1988). Such cleavage presumably represents the enhanced interaction of Int with the attachment site that occurs during synapsis. Thus, the cleavage assay not only can detect the Int binding to isolated attachment sites but can be used to assess communication between attachment sites.

Heteroduplexes of the bacterial attachment site

In previous work, little or no cleavage of *att*B heteroduplexes was detected after incubation with Int and IHF in the presence of non-specific DNA such as pBR322 (Richet *et al.*, 1988). From this result and related footprinting studies, we argued that the interaction of Int with *att*B is too weak

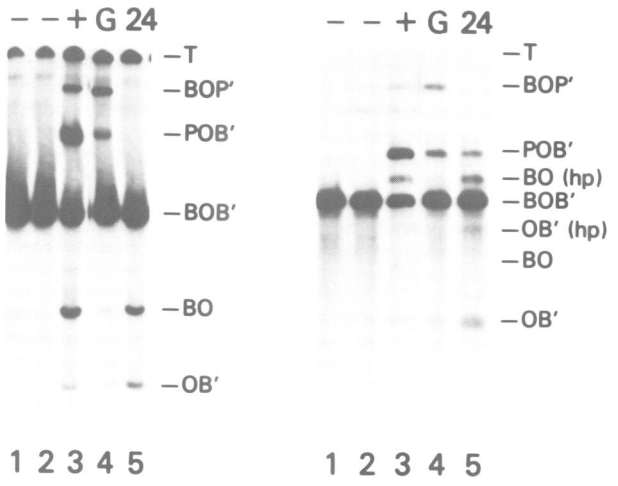

Fig. 2. Cleavage and strand transfer assays with an *att*B heteroduplex. An *att*B site (coordinate −570 to +390) was made by annealing the top strand of *att*B *saf*$^+$ and the bottom strand of *att*B *saf*G. The heteroduplex (3′-end labeled at both ends) was incubated as described in Materials and methods in the absence of recombination proteins (lane 1) or in the presence of IHF plus Int (lanes 2–5) with plasmids containing the following attachment sites: none (pBR322-**lanes 1** and **2**); *att*P wild type (pHN894-**lane 3**); *att*P*saf*G (pCF5-**lane 4**); *att*24 (pPH2401-**lane 5**). Subsequently, the reactions were stopped, restricted, split in half and electrophoresed [along with labeled size markers (not shown)] on a native acrylamide gel (left panel) or an alkaline agarose gel (right panel). At the right of each panel is indicated the position of the top of the gel (T), two recombinant products (BOP′ and POB′), the substrate heteroduplex (BOB′) and two Int cleavage products (BO and OB′). The denaturing gel (right panel) reveals that some cleavage products have the mobility expected for hairpins (hp).

to compete even with non-specific DNA. In those experiments the heteroduplex DNA was labeled at its 5′ ends and double-strand cleavage was assayed by native acrylamide gel electrophoresis. We have now increased the sensitivity of this assay in two ways. First, product analysis has been performed under both native and denaturing conditions; this permits detection of single-strand nicks introduced by Int as well as double-strand breaks. Second, the DNA has been labeled at its 3′ ends, thereby avoiding the complication of detecting fragments with Int covalently joined to the 3′ end (Craig and Nash, 1983; Pargellis *et al.*, 1988). Even with these improvements, no specific cleavage of an *att*B heteroduplex can be seen after incubation with Int and IHF (Figure 2, lanes 1 versus 2). Under these conditions, label is often seen trapped at the top of the native gel (see Figure 2, left panel). This does not appear to reflect specific binding of recombination proteins to the heteroduplex because in typical experiments the level of trapping is comparable when Int and IHF are omitted (cf. lane 1 versus 2). Taken together, these results confirm our previous conclusion about the weakness of Int's interaction with *att*B.

Our earlier study also showed that if pBR322 DNA is replaced by a plasmid containing a homoduplex *att*P, the interaction of Int with the *att*B heteroduplex is greatly stimulated (Richet *et al.*, 1988). As discussed above, the outcome of this interaction could be either recombination or double-strand cleavage. In the latter case, an unexpected result was that the cleaved product did not show evidence of covalently attached protein, suggesting the formation of hairpins (Figure 1B). Evidence in support of this suggestion is presented in Figure 2. In native gels, cleaved products migrate as expected for molecules that have been broken by

Int in the core region, thereby producing fragments of 570 and 390 bp containing the B and B′ arms, respectively (Figure 2, left panel, lane 5). However, in denaturing gels (Figure 2, right panel) a large fraction of these products migrate with apparent sizes of 1140 and 780 nt, precisely the result expected if the ends of the cleaved DNA were joined into a hairpin. In contrast, recombinant products behave consistently in native and denaturing gels (Figure 2, lanes 3 and 4). We have noted that omission of spermidine depresses the appearance of cleaved products as well as recombinants (data not shown). This suggests that polyamines, which are required for integrative recombination (Nash, 1975), are needed for an early step in the reaction and not just for strand exchange, a step which is presumably unnecessary for the cleavage assay.

Cleavage of *att*B heteroduplex is stimulated at least as well by *att*P24 a 1-bp deletion in the overlap region as by *att*P *saf*-2A, a 1 bp substitution (Figure 2 and data not shown). *att*P24 is an atypical *saf* mutant in that its recombination efficiency is low even when mated with an *att*B partner that contains the same mutation (Shulman and Gottesman, 1973). It seems plausible that *att*P24 is defective in recombination because of misalignment of Int protomers that are bound to the core region (Ross *et al.*, 1982). We previously showed that supercoiling, IHF and both arms of *att*P are needed to promote interaction with an *att*B heteroduplex (Richet *et al.*, 1988). In brief, it appears that only an ordered structure, the *att*P intasome, can capture *att*B. The success of *att*P24 in the *att*B cleavage assay suggests that either Int protomers bound to the core are not involved in the intasome or that their proper positioning is not essential for synapsis. We prefer the latter explanation because a hybrid *att*P with the left and right arms of the lambda attachment site but the core region from an attachment site with a different core specificity [that of phage HK022 (a gift from N.Ramaiah)] fails to promote the cleavage of *att*B heteroduplexes (unpublished observations).

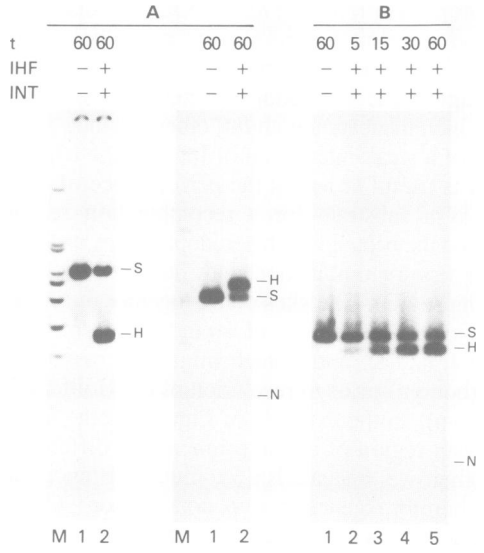

Fig. 3. Cleavage of *att*P heteroduplexes by IHF plus Int. (**A**) A heteroduplex *att*P site (coordinates −160 to +137) was made by annealing the top strand of *att*P *saf*$^+$ and the bottom strand of *att*P *saf*G. The resulting DNA (3′-end labeled at position −160) was incubated for 60 min in the presence of pBR322 DNA with Int plus IHF as indicated, split in half and loaded onto either a native acrylamide gel (**left panel**) or a denaturing agarose gel (**right panel**). At the right of each panel is indicated the position of the substrate heteroduplex (S) and the labeled Int cleavage products—a double-strand break (H), often joined into a hairpin, and a single-strand nick (N). The lanes marked M contain the end-labeled *Hin*fI digest of plasmid pPH54 (Hsu *et al.*, 1980); the fragment sizes (in bp) in the digest are: 1082, 517, 506, 396, 344, 317, 298, 297, 221, 220, 154 and 75. The 317 bp fragment contains *att*P; in the native acrylamide gel, it has an anomalous mobility (Ross *et al.*, 1982) and comigrates with the 344 bp fragment. (**B**) An *att*P *saf*$^+$/*saf*G heteroduplex (coordinates −115 to +137) was made as above. The heteroduplex (3′-end labeled at position −115) was incubated with Int and IHF for the indicated times and loaded on to a denaturing agarose gel.

Heteroduplexes of the phage attachment site

In contrast to the behavior of *att*B, heteroduplexes of *att*L are efficiently cleaved by Int even in the presence of non-specific DNA (Nash *et al.*, 1987a). From this result and supporting footprint experiments, we concluded that Int bound to the P′ arm of *att*L can assist the binding of Int to its core (Richet *et al.*, 1988). It is of interest to know whether the P arm alters the influence of the P′ arm, i.e. whether *att*P and *att*L display different Int cleavage behaviors. As shown in Figure 3A, just as with *att*L, heteroduplexes of *att*P are efficiently cleaved. This shows that the Int and IHF binding sites of the P arm do not greatly alter the effect of the P′ arm. Moreover, denaturing gel analysis (right panel of Figure 3A) indicates that the cleavage product is almost entirely processed into hairpins, i.e. the labeled 3′ end is 160 nt from the core but the cleavage product migrates as a 320 nt fragment. We have studied the structure of the hairpin in more detail using a derivative of *att*P in which the labeled end is closer to the core. Heteroduplexes of this derivative are also cleaved efficiently (Figure 3B). In this experiment, a close coupling between cleavage and resealing is demonstrated; even in short incubations the hairpin form predominates and little or no nicked intermediate is seen. When the nucleotide sequence of this hairpin is examined (Figure 4), the data not only confirm the hairpin nature of the cleaved product but support the interpretation that hairpins are formed by Int cleavage at the edges of the overlap region, i.e. at the places where Int promotes strand exchange during normal recombination. This indicates that, although Int topoisomerase is highly selective in initiating strand attack, it may be more catholic in its capacity for rejoining. Other topoisomerases create hairpins in DNA (van der Ende *et al.*, 1981; Greenstein and Horiuchi, 1989; Reddy and Bauer, 1989); perhaps this is the way crosslinks that are found at the ends of chromosomes (Barbour and Garon, 1987) and elsewhere (Alberts and Doty, 1968) are produced in nature.

In addition to Int and IHF binding sites, the P arm also contains binding sites for Xis (reviewed in Craig, 1988). We wondered whether this protein could alter the interaction of Int with the core. In the absence of published data on the effect of Xis on the occupancy of Int at the core of *att*P, we began our study by using two different footprinting techniques on a homoduplex *att*P. Dimethylsulfate (DMS) protection of the core by Int (Figure 5, lanes 1−4) was unperturbed by Xis. Neocarzinostatin (NCS) footprinting (Figure 5, lanes 5−9) also demonstrated that Int remains bound to the core in the presence of Xis (i.e. the region from −16 to +16 remained protected). However, the NCS footprint provided a hint that Xis alters the nucleoprotein array near the core; a significant enhancement of cleavage

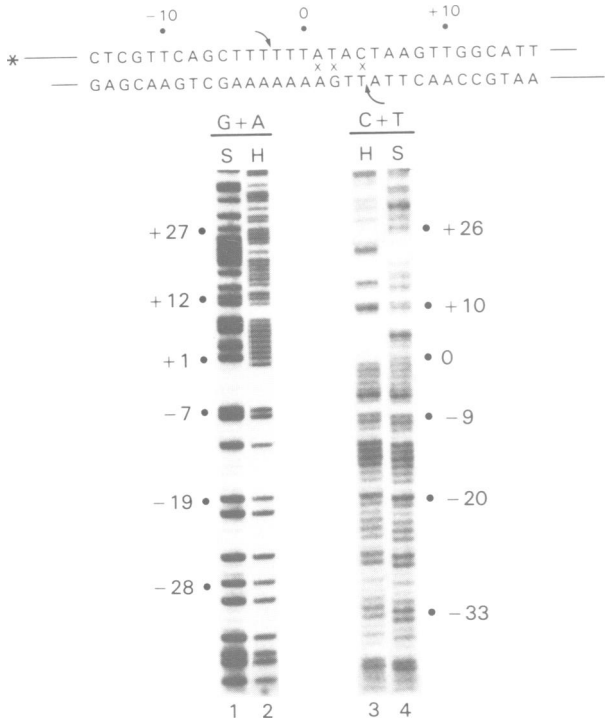

Fig. 4. Nucleotide sequence of a cleavage product. The same heteroduplex as used in Figure 3B was 5′ end-labeled at position −115, incubated for 1 h with IHF and Int, and electrophoresed through a native acrylamide gel. The major cleavage product was eluted and sequenced. At the **top** is shown the sequence of the substrate DNA (mismatches in the heteroduplex marked with x's) and the positions of the expected Int cleavages (marked with curved arrows). Joining the top and bottom strands at the sites of Int cleavage should generate a product whose sequence is identical to that of the substrate up to position 0 (rather than to position −2 because of the identity of the first two nt that are 3′ to the cleavage site in both top and bottom strands). The sequencing lanes compare substrate DNA (**S**) and cleaved product (**H**). Differences between these are seen to start at coordinate 0. At this point the hairpin should begin a run of nine purines. An A > C sequencing reaction (not shown) confirms that the diagnostic purine run has the expected sequence GA_7G.

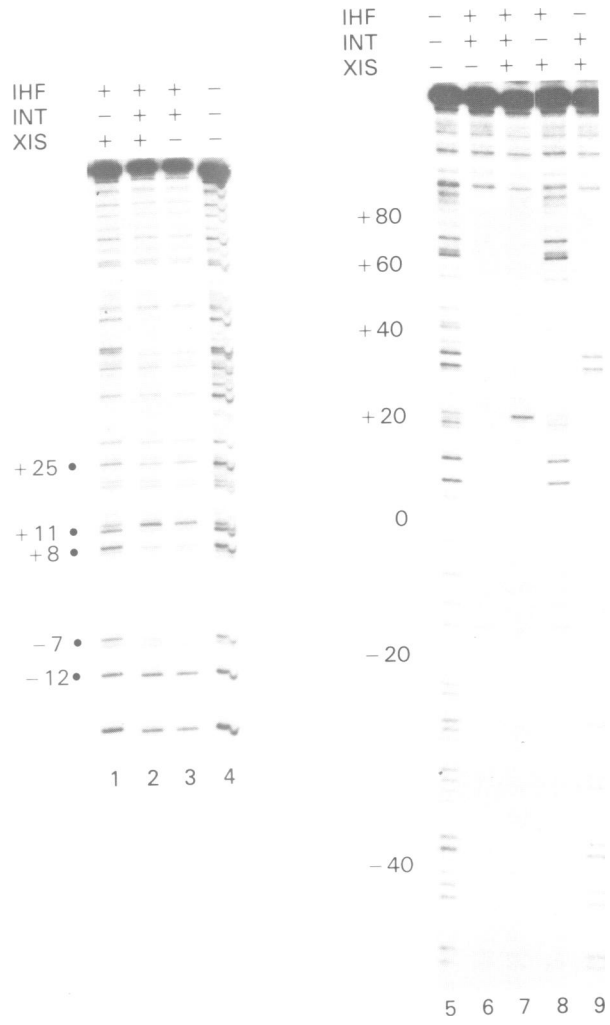

Fig. 5. Effect of Xis on the *att*P footprint. An *att*P homoduplex (coordinates −115 to +137), 5′-end labeled at its left end, was incubated with 6 U IHF, 0.4 U Int and 1 U of Xis in the indicated combinations; the mixture was then probed with DMS (**lanes 1–4**). Diagnostic features of the core footprint include enhancement of +12 (G) and protection of both +11 (G) and −7 (G). A second aliquot of the *att*P fragment was incubated with 6 U IHF, 2 U Int and 1 U of Xis as indicated and probed with NCS (**lanes 5–9**) as described in Materials and methods.

of a residue near coordinate +20 was consistently observed in the presence but not in the absence of Xis (Figure 5, lane 6 versus 7). The location of this enhancement, between the core binding site for Int and the H′ binding site for IHF, and the dependence of the enhancement on both IHF and Int (Figure 5, lanes 8 and 9) suggest that Xis bound to its sites in the P arm can influence contact between IHF and Int in the P′ arm.

We used the Int-promoted cleavage of an *att*P heteroduplex to test whether such subtle effects of Xis on the positioning of recombination proteins might have a functional consequence. We found that addition of Xis to IHF and Int causes a dramatic decrease in the efficiency of cleavage of the top strand of *att*P; hairpins are drastically reduced and few nicked molecules accumulate (Figure 6A, lane 4 versus 5). Analysis of a heteroduplex labeled in the bottom strand again showed a major reduction in formation of hairpins although a little nicked material accumulates (Figure 6B). Although this experiment was carried out with DNA that was truncated just to the left of the Xis binding site in *att*P, the same effect was seen with *att*P that carried a complete set of Int and IHF binding sites (−160 to +137; data not shown). The time course shown in Figure 6B rules out the possibility that Xis permits initial attack by Int but causes reversal of strand breaks at later times. We conclude that Xis depresses Int attack on *att*P. To our knowledge, this is the first demonstration that Xis perturbs the function of Int topoisomerase. We do not know if this perturbation is a consequence of direct interaction between Xis bound in the P arm and Int bound at the core or is an indirect consequence of Xis influence on IHF and/or Int bound in the arms of *att*P. The latter possibility is plausible because Xis bends DNA (Thompson and Landy, 1988) and thereby could disrupt a network of protein−protein interactions. Moreover, the capacity of Xis to depress cleavage of heteroduplexes is strongly dependent on IHF (Figure 6A). In any case, the capacity of Xis to influence Int cleavage does depend on its ability to bind to *att*P; we found little or no effect of Xis on the cleavage of a heteroduplex *att*L, an attachment site without a specific Xis binding site (data not shown).

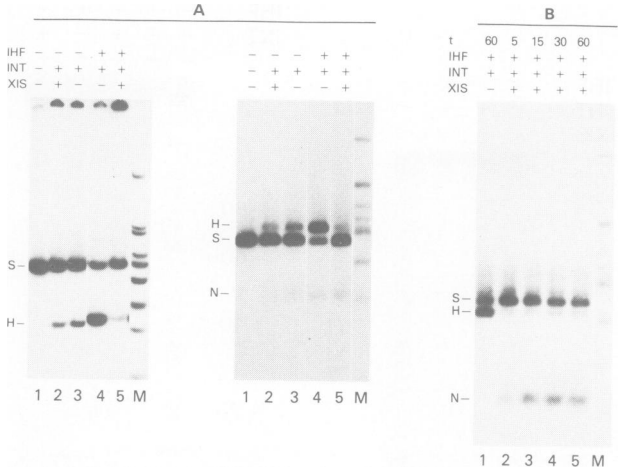

Fig. 6. Effect of Xis on cleavage of *att*P heteroduplexes. (**A**) An *att*P *saf*$^+$/*saf*G heteroduplex (coordinates −115 to +156), 3′-end labeled at position +156, was incubated in the presence of pBR322 DNA with IHF, Int and Xis in the indicated combinations, split in half and electrophoresed through a native acrylamide gel (**left panel**) or a denaturing agarose gel (**right panel**). (**B**) An *att*P heteroduplex like that in Figure 3B was 3′-end labeled at position −115 and incubated as above for the indicated times with IHF, Int and Xis. The mixture was electrophoresed through a denaturing agarose gel. Markers and identified bands are as in Figure 3.

The interaction of Int with the right-hand prophage attachment site

In the previous section we have examined the capacity of the P arm to modify the influence that the P′ arm has on the interaction of Int with the core. We next asked whether the P arm influences the core in the absence of the P′ arm. Recall that BOB′, the bacterial attachment site, interacts very weakly with Int (Figure 2; see also Richet *et al.*, 1988). We have asked if the replacement of B sequences by the P arm improves that interaction. Bushman *et al.* (1985) have shown that a functional *att*R (POB′) does not require all the binding sites found within the P arm. Specifically, the leftmost Int and IHF binding sites are dispensable. Accordingly, we began our studies using a derivative of *att*R that lacks these sites. As in earlier work, our footprinting assays are modeled on recombination reactions and contain Int plus IHF as well as supercoiled pBR322 DNA as a non-specific replacement for a recombination partner. As shown in Figure 7, under these conditions protection of the core of a homoduplex *att*R against attack by NCS can be detected (lane 4 versus 5). However, the footprint is notably weaker than that seen with *att*P (Figure 5); many bands within the core region are only partially protected and this protection requires higher levels of Int than are required for complete protection of the comparable region of *att*P. The footprint is reproducibly improved by the addition of Xis protein (lane 1 versus 5) but still requires high levels of Int. Even with derivatives of *att*R that contain an entire P arm, footprints of the core are still weak (data not shown). Indeed, under slightly different conditions Thompson *et al.* (1987) were unable to detect Int bound to the core of *att*R. We conclude that the P arm improves the affinity of Int for the core but this improvement is substantially less than that afforded by the P′ arm; DMS footprinting (data not shown) leads to the same conclusion.

An independent estimate of the capacity of Int to interact with the core of *att*R can be obtained using heteroduplexes.

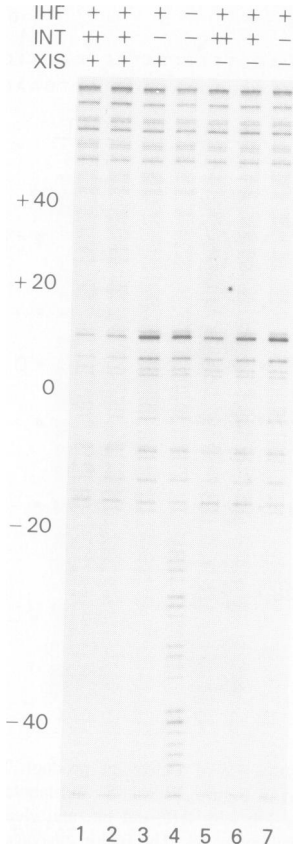

Fig. 7. Nuclease protection of the core of *att*R. A restriction fragment containing *att*R (coordinates −115 to +269), 5′-end labeled at its left end, was mixed with 6 U IHF, 1 U of Xis, and either 2 U or 6 U of Int as indicated (+ or ++, respectively); after 40 min the mixture was probed with NCS as described in Materials and methods.

Figure 8 shows that, in contrast to *att*P heteroduplexes, heteroduplexes of *att*R are cleaved very poorly when mixed with Int and IHF. Moreover, addition of Xis protein has opposite effects on *att*P and *att*R heteroduplexes, drastically inhibiting cleavage of the former but stimulating cleavage of the latter. Even under these optimal conditions (Figure 8, lane 3), the cleavage of *att*R heteroduplexes is only a little better than that seen for *att*B heteroduplexes (Figure 2, lane 2). Taken together with the footprinting data, it appears that the P arm does not promote effective binding of Int to the core. It is simplest to assume that, like *att*B, the core of *att*R can not obtain Int from solution but enters into synapsis with *att*L as a naked segment of DNA. Alternatively, the core of *att*R may bind Int but the protein is positioned poorly, rendering the complex weak and unable to initiate strand cleavage.

Effect of a recombination partner on attR heteroduplexes

Figure 9A shows that processing of an *att*R heteroduplex is greatly stimulated when a supercoiled *att*L plasmid replaces non-specific DNA in the reaction mixture. As with *att*B heteroduplexes, if the *att*L partner matches one strand of the heteroduplex, recombinants are found (lanes 7 and 8). But, with other *att*L *saf* variants, the predominant product is a double-strand break (lane 5 and 6). Analysis under denaturing conditions (Figure 9A, right panel) indicates that most of the cleaved DNA again is in the form of hairpins.

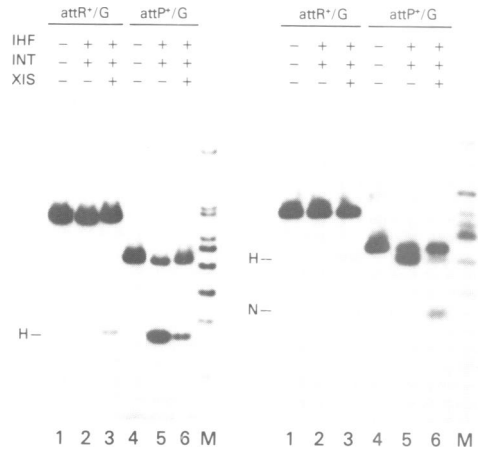

Fig. 8. Cleavage of *att*R and *att*P heroduplexes. An *attRsaf*$^+$/*saf*G heteroduplex (coordinates −115 to +269) and an *attPsaf*$^+$/*saf*G heteroduplex (coordinates −115 to +137), 3′-end labeled at their left ends, were incubated in the presence of pBR322 DNA for 60 min with IHF, Int and Xis as indicated. The mixtures were split in half and electrophoresed through a native acrylamide gel (**left panel**) or a denaturing agarose gel (**right panel**).

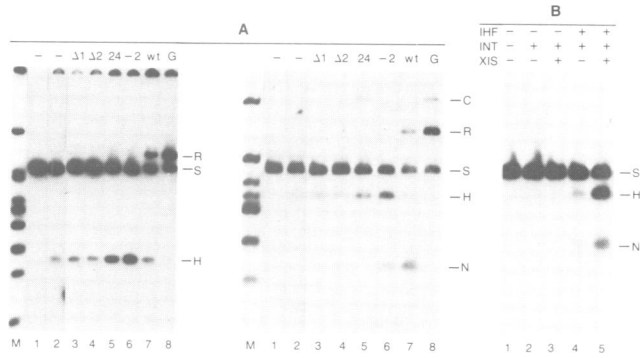

Fig. 9. Effect of recombination partners on an *att*R heteroduplex. (**A**) An *attRsaf*$^+$/*saf*G heteroduplex (coordinates −160 to +269), 3′-end labeled at its left end, was mixed in the absence of recombination proteins (**lane 1**) or with IHF, Int and Xis (**lanes 2–8**) in the presence of plasmids containing the following attachment sites: none (pBR322—**lanes 1** and **2**); *att*L deleted for the leftmost core binding site (pHN977—**lane 3**); *att*L deleted for both core binding sites (pHN976—**lane 4**); *att*L24 (pHN996—**lane 5**); *att*L *saf*-2A (pHN889—**lane 6**); *att*L *saf*$^+$ (pHN853—**lane 7**); *att*L *saf*G (pHN891—**lane 8**). Subsequently, the reactions were stopped, restricted, split in half and electrophoresed through a native acrylamide gel (**left panel**) or a denaturing agarose gel (**right panel**). Markers and identified bands are as in Figure 3 except that the position of the proper (R) and contrary (C) recombinants (see text) are also indicated. (**B**) The same *att*R heteroduplex as in (**A**) was incubated in the presence of *att*L *saf*-2A with the indicated combinations of IHF, Int and Xis, restricted and electrophoresed through a denaturing agarose gel.

What structural features of *att*L are essential for this stimulation? We performed a series of experiments in which *att*L was replaced by variants which lacked one or more binding sites for Int. Our results (lanes 2 and 3 and data not shown) indicate that *att*L must contain both the Int binding sites of the P′ arm (removed by deletion beyond coordinate +46) and the Int core binding sites (removed as described in Materials and methods), to be able to interact with *att*R. In contrast to integrative recombination, excisive recombination does not show a marked dependence on spermidine (unpublished observations) or supercoiling (Nunes-Düby *et al.*, 1987). Both features were also observed with assays of heteroduplex cleavage (data not shown). It should be emphasized that stimulated cleavage of *att*R heteroduplexes differs from standard excisive recombination in its lack of dependence upon homology within the overlap region. Variants of *att*L that differ from *att*R either at the left of the overlap region (lane 6), at the middle of the overlap region (*att*L +1G, data not shown), or by a 1-bp deletion (lane 5) all promote substantial stimulation of cleavage. This demonstrates that, just as for integrative recombination, synapsis between the partners of an excisive cross does not depend on matching of the overlap region; the requirement for homology must come into play at a later step.

It was of particular interest to examine the Xis-dependence of the interaction between *att*L and heteroduplexes of *att*R. We do not know how Xis facilitates the excisive reaction pathway. Perhaps Xis is needed only in the later steps of recombination, i.e. branch migration and/or resolution of Holliday structures. If this were the case, one would expect that cleavage of *att*R heteroduplexes, which involves only juxtaposition of *att*L with *att*R (and possibly formation of Holliday structures), would take place in the absence of Xis. However, Figure 9B shows that only a small amount of heteroduplex cleavage is observed without Xis (lane 4 versus 5); in this experiment, the amount of cleavage without Xis approximated that seen when the *att*L partner was replaced with pBR322 (data not shown). Thus, it appears that Xis is needed for an early step in the excision pathway. Similarly, the capacity of Xis to inhibit Int topoisomerase action on *att*P (Figure 6) may indicate that inhibition of integration by Xis (Nash, 1975; Abremski and Gottesman, 1982) also represents interference with a step prior to strand exchange.

Several of the reaction mixtures of Figure 9A showed a small amount of an unexpected band upon analysis in denaturing gels (right panel, lanes 5 and 8). The apparent molecular weight of this fragment suggested that it contained the labeled P arm of *att*R (160 nt) joined to the B arm of *att*L (952 nt), a hypothesis supported by an appropriate change in mobility of this fragment when different restriction enzymes were used to cut the B arm (data not shown). The absence of a corresponding band after electrophoresis in a native gel (left panel) suggested that some partial recombinant was being produced. We first asked whether this anomalous product was unique to recombination with heteroduplexes. Figure 10A shows that none of the product is seen under identical conditions with a homoduplex substrate. Indeed, Figure 10A confirms that homoduplex *att*R is not processed in a detectable way when mixed with *att*L *saf* partners. The dull pattern that is seen with homoduplex substrates—simple recombination with a homologous partner and no products with a non-homologous partner—highlights the novelty and utility of the heteroduplex substrates. We next examined the behavior of a second *att*R heteroduplex, one in which the top and bottom strands of the overlap region contained *saf*G and *saf*+ information respectively (i.e. the converse of the heteroduplex used in Figure 9). The same spectrum of processed products was observed (Figure 10B), confirming our previous conclusion about the role of homology in the early steps of excision. However, the proportions of these products were different; most notably, double-strand cleavage was rarer but the anomolous recombinant was present in substantial levels (lanes 4 and 5). This facilitated further study, in which it

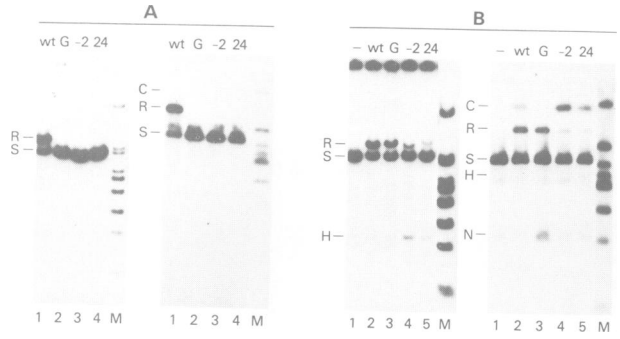

Fig. 10. Comparison of an *att*R homoduplex and heteroduplex as recombination substrates. (**A**) An *att*R *saf*$^+$/*saf*$^+$ homoduplex and (**B**) an *att*R*saf*G/*saf*$^+$ heteroduplex (coordinates −160 to +269), 3′-end labeled at their left ends, were incubated with IHF, Int and Xis in the presence of the indicated plasmids containing either no attachment site (pBR322, lanes marked −), *att*L *saf*$^+$ (pHN853, lanes marked wt), *att*L*saf*G (pHN891, lanes marked G), *att*L-2A (pHN889, lanes marked −2), or *att*L24 (pHN996, lanes marked 24). The reactions were treated as in Figure 9 and electrophoresed either through a native acrylamide gel (**left panel**) or a denaturing agarose gel (**right panel**).

was found that the unusual product depended upon Xis as well as Int and IHF, was not produced when *att*L was replaced by *att*R or *att*B, and had a mobility which was unaffected by proteinase digestion (data not shown). We then obtained DNA sequence information from this product. The data of Figure 11 not only confirm that the P arm is joined to the B arm but show that the joining takes place at the normal positions of Int cleavage. Because the genetic polarity of this unusual recombinant is opposite to that normally seen during site-specific recombination (i.e. the bottom strand of the P arm is connected not to the bottom strand of the B′ arm but to the top strand of the B arm), we have named this product a 'contrary' recombinant. Using 'half attachment sites', Nunes-Düby *et al.* (1989) have discovered a similar product.

Discussion

Since their introduction by Bauer *et al.* (1984), hetroduplex attachment sites have proven to be a very useful tool for investigating the mechanism of lambda site-specific recombination. They have been a key part of the critical experiments that eliminated synapsis as the step which requires perfect matching between attachment sites (Richet *et al.*, 1988). Moreover, as diagrammed in Figure 1, the pattern of their success in replacing homoduplex sites has provided strong evidence in favor of branch migration as the key homology-dependent step in recombination (Bauer *et al.*, 1985; Nash *et al.*, 1987a). In the present work, we have used heteroduplex sites to reveal several different aspects of the integration-excision system. The different efficiencies of cleavage of heteroduplexes has indicated that attachment sites fall into two classes with respect to the functional interaction of their cores with Int protein—strong (*att*L and *att*P) and weak (*att*B and *att*R). This classification could mean that both integration and excision pathways depend upon the capture of naked core DNA by a nucleoprotein complex formed on the partner site. Moreover, the double strand cleavage of *att*L and *att*P heteroduplexes that is seen in the absence of a recombination partner shows that Int can cleave both the top and bottom strands without strand exchange. If this happens during normal recombination, the

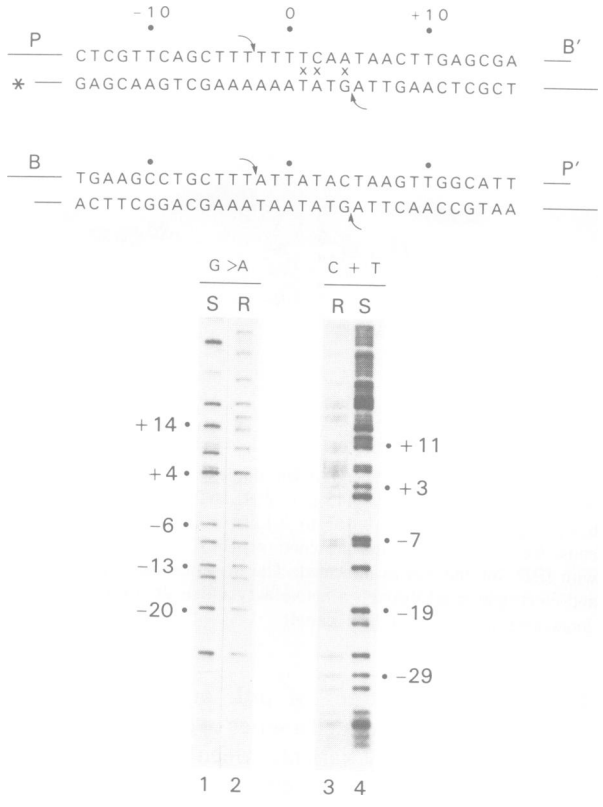

Fig. 11. DNA sequence of a contrary recombinant. The recombination reaction between *att*L*saf*-2A and a 3′-end labeled *att*R*saf*G/*saf*$^+$ heteroduplex like that of Figure 10B, lane 4 was scaled up 10-fold. The unusual recombinant band was excised from a denaturing agarose gel, electroeluted and sequenced as described in Materials and methods. At the top is shown the sequence of the substrates in the cross; an asterisk marks the point of the end-label in *att*R and the arrows indicate the expected positions of Int cleavage and strand exchange. Joining the bottom strand of *att*R to the top strand of *att*L should generate a product whose sequence is identical to that of the labeled substrate up to position +4; at this point the recombinant should acquire the sequence 5′ TTTCGTCC. . .3′. The sequencing lanes compare substrate (S) and the recombinant product (R); the expected pattern is found.

ordered sequence of strand exchange, top strands before bottom (Nunes-Düby *et al.* 1987; Kitts and Nash, 1988), would then depend on ordering of strand transfer, not strand cleavage. Heteroduplexes have also provided some clues about the way Xis protein controls directionality. The dramatic depression of Int cleavage of an *att*P heteroduplex suggests that Xis can inhibit integrative recombination by modifying the interaction of Int with the core region; footprinting studies show that the modifications must be subtle. Moreover, heteroduplexes have provided the first evidence against the possibility that Xis is needed only for late steps, such as branch migration or resolution of Holliday structures, in the excision pathway.

One of the most surprising findings to emerge from our studies of heteroduplex substrates is a novel recombinant product (Figure 11) in which strands from two parents have been joined into a 'contrary' structure with normal chemical polarity but with reversed genetic polarity. In understanding how such an event might arise, two observations seemed important. First, the recombinant was incomplete, i.e. it was not observed as a double-stranded DNA in which both strands of each parent had recombined to generate a contrary

product but was seen only when individual strands were analyzed on denaturing gels. Second, contrary recombination was observed only with heteroduplex substrates. Consideration of these facts led to the formulation of the model shown in Figure 12. We propose that juxtaposition of attachment sites and initial attack by Int is normal (panel A). It should be recalled that excisive recombination normally begins by attack of the top strands of *att*L and *att*R; this is followed by reciprocal exchange of strands to make a Holliday junction (Nunes-Düby *et al.*, 1987; Kitts and Nash, 1988). We propose that in the pathway leading to contrary recombinants, one of the reciprocal joins fails to occur. It seems reasonable to imagine that this happens because, without the constraint of Watson–Crick pairing, one cleaved 5′ hydroxyl end drifts away from its proper position (panel B). Note that Int remains covalently attached to the 3′ phosphate end of the unjoined strand (Craig and Nash, 1983; Pargellis *et al.*, 1988). The critical event for generating contrary recombinants occurs when Int attacks the bottom strand. As shown in panel C, cleavage of the heteroduplex attachment site creates a double-strand break. Now there are two strands with covalently attached Int protein and two strands with free 5′ hydroxyl ends. There are two ways in which strand rejoining can occur. One leads to a normal Holliday junction (not shown); panel D shows the set of connections that produces a contrary recombinant. In this case, just as in the experiments described in the previous section, a recombinant strand has been produced that runs from a 3′ end in the P arm to a 5′ end in the B arm. Thus, the model accounts for the sequence determined in Figure 11. Note that the model also makes predictions about other consequences of strand exchange i.e. both a hairpin and a proper recombinant strand should be produced. We have tested these predictions: an *att*R *saf*G/*saf*$^+$ heteroduplex was differentially labeled so as to follow each part of the attachment site, recombined with an *att*L *saf*-2A and analyzed on a denaturing gel (data not shown). When the P arm was 5′-end labeled, only a proper recombinant strand was seen and when the B′ arm was either 5′ or 3′-end labeled, only hairpins were seen. Thus, the pattern of products oberved in this cross exactly corresponds to that predicted by the model of Figure 12. Moreover, in each case the amount of product was comparable to that expected from the yield of contrary recombinant when the P arm was 3′-end labeled (Figure 10B). It should be mentioned that we have also observed contrary recombinants during integrative recombination. As with excisive recombination, these products were observed only with heteroduplex substrates. Although all the predictions of Figure 12 have not been tested in the case of integrative recombination, we believe the same model applies.

One feature of these unusual reactions that remains puzzling is the way their efficiency depends upon the particular heteroduplex used. The *saf*$^+$/*saf*G and *saf*G/*saf*$^+$ heteroduplexes have the same number of mismatches but give reproducibly different proportions of processed products. It is clear that different mismatches have different conformations and cause different distortions of the double helix (Hunter *et al.*, 1987). We believe that these differences dictate the relative efficiency of each processing pathway but we do not understand the critical feature that leads in one case to strand transfer to a recombination partner and in the other case to hairpin formation.

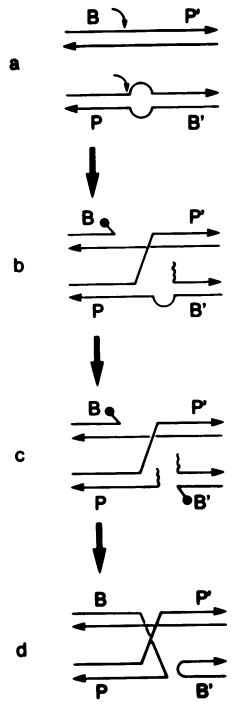

Fig. 12. A model for contrary recombination. (**A**) A homoduplex *att*L (BOP′) and a heteroduplex *att*R (POB′) are shown juxtaposed in a synaptic structure. The 3′-end of each strand is indicated by an arrowhead; the curved arrows show the points of Int cleavage on the top strands of each site. (**B**) An abortive strand transfer has created one recombinant strand but has left Int topoisomerase covalently joined to the B side of the core of *att*L. (**C**) Int topoisomerase attack on the bottom strand of the *att*R heteroduplex breaks this attachment site into two pieces. (**D**) The Int-promoted reunion of DNA has created a hairpin and a structure with three arms. One of the strands of this Y structure is the contrary recombinant described in the text and Figure 11.

Int protein belongs to a family of site-specific recombinases that are related by structural and functional aspects of strand exchange (Argos *et al.*, 1986; Craig, 1988). Recently, Cox and coworkers have made observations on one member of this family, the yeast FLP protein, that are reminiscent of our findings concerning contrary recombination (Meyer-Leon *et al.*, 1988). They prepared homoduplex substrates with overlap regions whose sequence was markedly different from that of the naturally occurring recombination target. When both partners in a cross had this sequence, recombination was inefficient, implying a need for certain structural features in the region in addition to homologous matching. Under these conditions, novel products were observed. When characterized by electron microscopy, these proved to be molecules with three arms joined in the overlap region. Linear duplexes whose strands were joined into hairpins at the overlap region were also found. These products, a Y form and a hairpin duplex are precisely the structures we observe during contrary recombination. Meyer-Leon *et al.* (1988) suggest that Y forms and hairpins arise during recombination when a standard Holliday junction is formed but processed such that one of its four arms is cut off and the resulting strand breaks are sealed. Although this proposal could also account for our observations, we favor the model of Figure 12 because it specifically explains how mismatched base pairs might prompt contrary recombination. Indeed, the data of Meyer-Leon *et al.* (1988) could also be

accommodated by our model. We note that Y structures were seen by them when the overlap region was palindromic and the substrate was supercoiled, two conditions that would favor the formation of stem-loop structures which might resemble the non-Watson–Crick regions in our heteroduplex substrates.

Regardless of its detailed mechanism of formation, contrary recombination is of interest because it provides strong support for the hypothesis (first raised by the formation of hairpins) that Int topoisomerase can be indiscriminate when choosing partners for rejoining. This lack of selectivity suggests a possible connection between the mechanism of conservative site-specific recombination and the mechanism of immunoglobulin gene rearrangements. The joining of V, D, and J segments in immunoglobulin and T cell antigen receptors clearly is a kind of site-specific recombination (Tonegawa, 1983) but the relationship between substrates and products in this system has made it seem remote from the Int family. Here, if one aligns two attachment sites so that both overlap regions read the same from left to right (parallel alignment), recombination can be viewed as the joining of the head of one site to the tail of the other. But if the same alignment is made with the signal sequences of the immunoglobulin family, the standard products are made by joining the head of one parent to the head of the other. Recently, Gellert and coworkers have found that head to tail joining occurs at a modest frequency in this system (Lewis *et al.*, 1988). Similarly, the existence of contrary recombinants shows that Int can carry out head to head joining. That is to say, both the lambda and the immunoglobulin systems can achieve both kinds of joining. Although there are clear differences in the efficiency and reciprocality of these processes, it may mean that the strand transfer process in the immunoglobulin system has some features in common with the well characterized lambda system.

Materials and methods

DNA and proteins

Supercoiled plasmid DNA was isolated and purified from an *E.coli rec*A mutant as described (Craig and Nash, 1983). *att*P and *att*L were cloned, respectively, as *Hin*dIII (−250) to *Bam*HI (+242) and *Eco*RI (−952) to *Bam*HI (+242) fragments which replaced the corresponding segments of pBR322. (The coordinate system for attachment sites is the center of the core region; in this frame, the overlap region has coordinates −4 to +2.) The sequence of the attachment site *saf* variants used in this paper is given in Kitts and Nash (1987). The *att*24 mutant is a deletion that reduces by 1 the string of six consecutive T residues in the core (Ross *et al.*, 1982). A plasmid containing the *att*P24 variant has been described (Ross *et al.*, 1982); a similar plasmid containing the *att*L24 variant was generated from a restriction digest of λ*att*^{2}LR24-24 phage (Shulman and Gottesman, 1973). A plasmid with an *att*L deleted for one core site (pHN977) was made by cloning the *Rsa*I (+1) to *Bam*HI (+242) fragment of *att*P *saf*+1G (Kitts and Nash, 1987) between the *Eco*RV and *Bam*HI sites of pBR322. A plasmid with an *att*L deleted for both core sites (pHN976) was made by cloning the *Sph*I (+29) to *Bam*HI (+242) fragment of pCB19 (Kitts and Nash, 1988) into the corresponding sites of pBR322. Single-stranded DNA was purified by standard methods from M13 phage grown as described (Bauer *et al.*, 1985). *att*B cloned in M13 as the *Hin*cII (−552) to *Hin*cII (+372) fragment has been described (Bauer *et al.*, 1985). *att*R was cloned into M13mp10 and M13mp11 either as the *Hin*dIII (−250) to *Bam*HI (+751) fragment as described (Nash *et al.*, 1987a) or as a *Hin*dIII (−160) to *Bam*HI (+751) fragment. In the latter case, the P arm contained an artificial *Hin*dIII site (Hsu *et al.*, 1980). This site was also used in the cloning of *att*P as a *Hin*dIII (−160) to *Bam*HI (+242) fragment which replaced the corresponding segment of M13mp10 and M13mp11. For all M13 clones, both the *saf*$^+$ and *saf*G variants of each attachment site were cloned in both orientations.

IHF protein was purified as described from the overproducing strain K5746 (Nash *et al.*, 1987b); in some experiments we used IHF that had been additionally passed through a phenyl-sepharose column in order to remove a minor endonuclease contaminant. Int was purified as described from HN695 (Nash *et al.*, 1987a). Xis was purified by a modification of the procedures of Better *et al.* (1983) and Abremski and Gottesman (1982) from strain KA1322 (Abremski and Hoess, 1983). One unit of each protein is defined as the amount needed to produce a saturated recombination reaction in the presence of optimal amounts of the other two proteins. Typically, one unit contained about 1.5 ng of IHF, 50 ng of Int, and 7 ng of Xis but these amounts varied at least 2-fold between batches of protein and upon storage.

Construction and labeling of fragments

Typically, fragments containing the attachment sites were made by annealing 50 μg each of two single-stranded DNAs from M13 derivatives that carried the top and bottom strands of an attachment site. Annealing was performed in 10 mM Tris (pH 8.0), containing 50 mM NaCl and 10 mM $MgCl_2$ in a volume of 200–500 μl. The sample was heated to 65°C and allowed to cool for about 2 h at 37°C; restriction enzyme (~150 units) was added and the mixture was digested for 1 h at 37°C and then treated with 2 units of calf intestinal alkaline phosphatase for 30 min. After heating to 70°C, the samples were electrophoresed through a 5% native acrylamide gel at 2 V/cm. The fragments were identified after ethidium bromide staining, eluted by soaking the crushed gel overnight and purified by absorption to a 0.2 ml DE52 (Whatman) column. After elution and ethanol precipitation, the samples were end-labeled (sp. act. = 3000 C/nmol) by treatment with polynucleotide kinase or the Klenow fragment of DNA polymerase I according to standard protocols (Maniatis *et al.*, 1982). After phenol extraction and ethanol precipitation, the labeled DNA was usually restricted so that the end without an attachment site migrated more rapidly than any of the products from the other labeled end.

Assays for cleavage and strand transfer

A standard (0.02 ml) reaction contained 50 mM sodium cacodylate (pH 8.0), 10.5 mM Tris HCl (pH 7.6), 0.4 mM sodium EDTA, 70 mM KCl, 5 mM spermidine, 225 μg/ml bovine serum albumin, 12.5 μg/ml of plasmid DNA (pBR322 or a derivative containing an attachment site), ~4000 c.p.m. of a labeled attachment site fragment and various combinations of recombination proteins. Unless otherwise stated 6 U of IHF, 2 U of Int and 1 U of Xis were used. Typically, cleavage and strand transfer reactions were prepared at 2.25 times the standard volume with all components increased proportionally. The mixture was incubated at 25°C for 60 min and stopped by heating to 70°C for 5 min. Assays for cleavage were then adjusted to 25 mM with sodium EDTA and split in half. Assays for strand transfer were adjusted to 10 mM $MgCl_2$ plus 50 mM NaCl and incubated with 3 units of various restriction enzymes for 60 min at 37°C before addition of EDTA as above. The restriction enzymes were chosen so as not to cut the labeled attachment site fragment and to cut the P arm of *att*P 1104 bp to the left of the core (*Ase*I), the B arm of *att*L 952 bp to the left of the core (*Eco*RI) and the P′ arm of *att*L 517 bp to the right of the core (*Sal*I). One of the divided aliquots was adjusted to 5% Ficoll (Pharmacia), 0.4% SDS and bromophenol blue to color and was loaded on a 5% polyacrylamide gel. The other aliquot was adjusted to 50 mM NaOH, 1 mM EDTA, 2.5% Ficoll and 1.6 mg/ml bromocresol green and was loaded onto a 3% or 4% NuSiev (FMC Co.) gel prepared as described (Maniatis *et al.*, 1982). The polyacrylamide gel was run in 90 mM Tris–borate containing 1 mM EDTA at 2 V/cm; the gel was then dried and autoradiographed. The agarose gel was run in 30 mM NaOH and 1 mM EDTA at 2 V/cm with buffer recirculation. The gel was pre-soaked in the running buffer for at least 2 h; this buffer was discarded and replaced with fresh running buffer before loading the samples. (Without this latter precaution, hairpin molecules often migrated anomalously.) After electrophoresis, the gel was neutralized, dried and autoradiographed.

Footprinting assays and DNA sequence determination

DMS footprinting assays were identical to the standard cleavage and strand transfer assay except that they contained ~15 000 c.p.m. of labeled attachment site; they were typically performed in a volume of 0.02 ml using pBR322 as the plasmid DNA. After 40 min at 25°C, 1 μl of a 20-fold dilution of DMS in ethanol was added; 3 min later the reaction was stopped by addition of 100 μl of chloroform–isoamyl alcohol (24:1). The aqueous phase was precipitated with ethanol and electrophoresed in a 8% sequencing gel as described (Craig and Nash, 1983).

Because of inefficient cleavage by NCS under our standard conditions, NCS footprinting assays required a slight modification of the reaction mixture. A typical reaction (0.02 ml) contained 54.5 mM Tris–HCl (pH 7.5), 70 mM KCl, 1.3 mM sodium EDTA, 10 mM β-mercaptoethanol, 11% glycerol, 225 μg/ml bovine serum albumin, 12.5 μg/ml of pBR322 DNA, 10 000–20 000 c.p.m. of labeled attachment site fragment, and

various amounts of IHF, Int and Xis. The reactions were stopped and processed as above.

DNA sequence determination used the rapid modification of the Maxam–Gilbert procedure (Bencini *et al.*, 1984).

Acknowledgements

We thank S.Nunes-Dünby and A.Landy for communication of results prior to publication, and G.Smith for sharing with us his preliminary sequence of *att*B. We acknowledge J.Gardner, A.Landy, and N.Ramaiah for DNA samples and bacterial strains. We are grateful to R.Weisberg, K.Mizuuchi, S.Nunes-Düby, A.Granston and G.Smith for their comments on this manuscript and to S.Means for preparing it.

References

Abremski,K.and Gottesman,S. (1982) *J. Biol. Chem.*, **257**, 9658–9662.
Abremski,K. and Hoess,R. (1983) *Gene*, **25**, 49–58.
Alberts,B.M. and Doty,P. (1968) *J. Mol. Biol.*, **32**, 379–403.
Argos,P., Landy,A., Abremski,K., Egan,J.B., Haggard-Ljungquist,E., Hoess,R.H., Kahn,M.L., Kalionis,B., Narayana,S.V.L., Pierson,L.S., III, Sternberg,N. and Leong,J.M. (1986) *EMBO J.*, **5**, 433–440.
Barbour,A.G. and Garon,C.F. (1987) *Science*, **237**, 409–411.
Bauer,C.E., Hesse,S.D., Gardner,J.F. and Gumport,R.I. (1984) *Cold Spring Harbor Symp. Quant. Biol.*, **49**, 699–705.
Bauer,C.E., Gardner,J.F. and Gumport,R.I. (1985) *J. Mol. Biol.*, **181**, 187–197.
Bencini,D.A., O'Donovan,G.A. and Wild,J.R. (1984) *BioTechniques*, **2**, 4–5.
Better,M., Wickner,S., Auerbach,J. and Echols,H. (1983) *Cell*, **32**, 161–168.
Bushman,W., Thompson,J.F., Vargas,L. and Landy,A. (1985) *Science*, **230**, 906–911.
Campbell,A.M. (1962) *Adv. Genet.*, **11**, 101–145.
Craig,N.L. (1988) *Annu. Rev. Genet.*, **22**, 77–105.
Craig,N.L. and Nash,H.A. (1983) *Cell*, **35**, 795–803.
de Massy,B., Dorgai,L. and Weisberg,R.A. (1989) *EMBO J.*, **8**, 1591–1599.
Greenstein,D. and Horiuchi,K., (1989) *J. Biol. Chem.* **264**, 12627–12632.
Hsu,P.L. and Landy,A. (1984) *Naure*, **311**, 721–726.
Hsu,P.L., Ross,W. and Landy,A. (1980) *Nature*, **285**, 85–91.
Hunter,W.N., Brown,T., Kneale,G., Anand,N.N., Rabinovich,D. and Kennard,O. (1987) *J. Biol. Chem.*, **262**, 9962–9970.
Kitts,P.A. and Nash,H.A. (1987) *Nature*, **329**, 346–348.
Kitts,P.A. and Nash,H.A. (1988) *J. Mol. Biol.*, **204**, 95–107.
Lewis,S.M., Hesse,J.E., Mizuuchi,K. and Gellert,M. (1988) *Cell*, **55**, 1099–1107.
Maniatis,T., Fritsch,E.F. and Sambrook,J. (1982) *Molecular Cloning, A Laboratory Manual*. Cold Spring Harbor Laboratory Press, Cold Spring Harbor, NY.
Meyer-Leon,L., Huang,L.C., Umlauf,S.W., Cox,M.M. and Inman,R.B. (1988) *Mol. Cell Biol.*, **8**, 3784–3796.
Moitoso de Vargas,L., Pargellis,C.A., Hasan,N.M., Bushman,E.W. and Landy,A. (1988) *Cell*, **54**, 923–929.
Nash,H.A. (1975) *Proc. Natl. Acad. Sci. USA*, **72**, 1072–1076.
Nash,H.A., Bauer,C.E. and Gardner,J.F. (1987a) *Proc. Natl. Acad. Sci. USA*, **84**, 4049–4053.
Nash,H.A., Robertson,C.A., Flamm,E., Weisberg,R.A. and Miller,H.I. (1987b) *J. Bacteriol.*, **169**, 4124–4127.
Nunes-Düby,S.E., Matsumoto,L. and Landy,A. (1987) *Cell*, **50**, 779–788.
Nunes-Düby,S.E.,Matsumoto,L. and Landy,A. (1989) *Cell*, in press.
Pargellis,C.A., Nunes-Düby,S.E., Moitoso de Vargas,L. and Landy,A. (1988) *J. Biol. Chem.*, **263**, 7678–7685.
Reddy,M.K. and Bauer,W.R. (1989) *J. Biol. Chem.*, **264**, 443–449.
Richet,E., Abcarian,P. and Nash,H.A. (1988) *Cell*, **52**, 9–17.
Robertson,C.A. and Nash,H.A. (1988) *J. Biol. Chem.*, **263**, 3554–3557.
Ross,W., Shulman,M. and Landy,A. (1982) *J. Mol. Biol.*, **156**, 505–529.
Shulman,M. and Gottesman,M. (1973) *J. Mol. Biol.*, **81**, 461–482.
Thompson,J.F. and Landy,A. (1988) *Nucleic Acids Res.*, **16**, 9687–9705.
Thompson,J.F., Moitoso de Vargas,L., Skinner,S.E. and Landy,A. (1987) *J. Mol. Biol.*, **195**, 481–493.
Tonegawa,S. (1983) *Nature*, **302**, 575–581.
van der Ende,A., Langeveld,S.A., Teertstra,R., van Arkel,G.A. and Weisbeek,P.J. (1981) *Nucleic Acids Res.*, **9**, 2037–2053.
Weisberg,R.A., Enquist,L.W., Foeller,C. and Landy,A. (1983) *J. Mol. Biol.*, **170**, 319–342.
Weisberg,R.A. and Landy,A. (1983) In Hendrix,R.W., Roberts,J.W., Stahl,F.W. and Weisberg,R.A. (eds), *Lambda II*. Cold Spring Harbor Laboratory Press, Cold Spring Harbor, NY, pp. 211–250.

Received on June 26, 1989